ACS OMEGA

http://pubs.acs.org/journal/acsodf

Article

First-Principles Investigation of Adsorption Behaviors and Electronic, Optical, and Gas-Sensing Properties of Pure and Pd-Decorated GeS_2 Monolayers

Ruilin Gao, Yongliang Yong,* Xiaobo Yuan, Song Hu, Qihua Hou, and Yanmin Kuang

Cite This: *ACS Omega* 2022, 7, 46440−46451

Read Online

ACCESS | Metrics & More | Article Recommendations | Supporting Information

ABSTRACT: The extensive applications of two-dimensional (2D) transition metal disulfides in gas sensing prompt us to explore the adsorption, electronic, optical, and gas-sensing properties of the pure and Pd-decorated GeS_2 monolayers interacting with NO_2, NO, CO_2, CO, SO_2, NH_3, H_2S, HCN, HF, CH_4, N_2, and H_2 gases by using first-principles methods. Our results showed that the pure GeS_2 monolayer is not appropriate to develop gas sensors. The stability of the Pd-decorated GeS_2 (Pd-GeS_2) monolayer was determined by binding energy, transition state theory, and molecular dynamics simulations, and the Pd decoration has a significant effect on adsorption strength and the change in electronic properties (especially electrical conductivity). The Pd-GeS_2 monolayer-based sensor has relatively high sensitivity toward NO and NO_2 gases with moderate recovery time. In addition, the adsorption of NO and NO_2 can conspicuously change the optical properties of the Pd-GeS_2 monolayer. Therefore, the Pd-GeS_2 monolayer is predicted to be reusable and a highly sensitive (optical) gas sensing material for the detection of NO and NO_2.

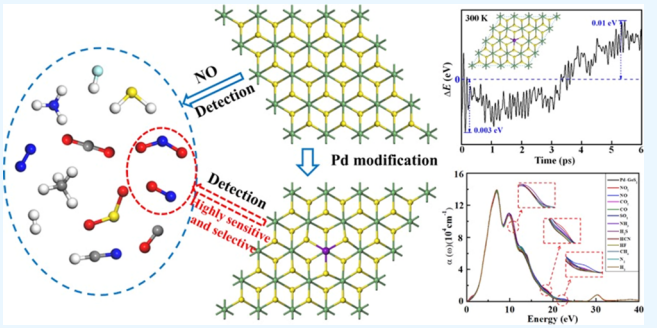

1. INTRODUCTION

Since its discovery in 2004, graphene has presented many fascinating properties, but its zero band-gap feature critically limits its myriad of applications in transistors, electronics, photonics, etc.[1−4] Although the modification of graphene can effectively open its band gap, this also reduces the electronic quality of the material, which is impractical for device applications.[5−7] This situation has stimulated scientists to design and investigate two-dimensional (2D) materials with semiconducting properties. Researchers have directed their studies to materials with layered honeycomb structures similar to that of graphite.[8−18] One of the most widely studied classes of these materials is 2D transition metal disulfides (TMDs).[19−21] 2D TMDs, which are nanomaterials in the formula of MX_2, M are TM atoms, such as Mo, W, and Ge, sandwiched between two X atoms (i.e., VIA group like S, Se, and Te), are structurally similar to graphene (i.e., owning hexagonal structures), but compensate for the zero band-gap of graphene. The participation of TM d-electrons with different numbers makes 2D TMDs exhibit different electrical properties, such as semiconducting with band-gap widths of about 1−2 eV, metallic, semiconductivity, and charge density wave behaviors, and thus have attracted remarkable interest for their potential applications in field-effect transistors, gas sensors, optical sensors, lubricants, etc.[22−24]

Since gas sensors have widely penetrated every aspect of our daily lives, such as medical and food industries and environmental safety testing,[25−29] 2D TMDs are ideal gas sensing materials due to their large specific surface-to-volume ratios, high sensitivity to adsorption of gases, which are available for interactions with gas molecules, abundant active sites to selectively bind gases, and good mechanical properties.[30−38] As one of the most common air pollutants, NO_x (x = 1 and 2), which are mainly from the combustion of fossil fuels, are greatly harmful to the environment and human health such as the damage of human respiratory organs and nerves.[8,9] Therefore, the development and manufacture of highly sensitive and selective NO_x gas sensors is a main challenge for monitoring air quality, especially, for the detection of NO_x at parts per billion (ppb) levels for commercial applications in environmental monitoring and healthcare.

As a TMD material with a large specific surface area, the GeS_2 monolayer with a sandwich-like structure has interesting physicochemical properties, such as excellent electronic

Received: August 10, 2022
Accepted: November 24, 2022
Published: December 8, 2022

https://doi.org/10.1021/acsomega.2c05142
ACS Omega 2022, 7, 46440−46451

transport properties and a high lattice thermal conductivity of 5.71 Wm^{-1} K^{-1} at 500 K.[39] For example, the CdI_2-type GeS_2 monolayer with an octahedral 1 T ($P\bar{3}m1$ space group) crystal structure was recently concluded to be a promising thermoelectric material due to its highest peak EFF value.[40,41] Although the synthesis of the CdI_2-type GeS_2 monolayer with an octahedral 1 T crystal structure (GeS_2 monolayer for short) has not been completed experimentally, phonon dispersion and ab initio molecular dynamics simulations have confirmed its thermodynamic and dynamic stabilities at 500 K.[39−41] These features make the GeS_2 monolayers have good potential in gas sensing. Here, analysis of the adsorption and electronic, optical, and gas-sensing properties of gas molecules (NO_2, NO, CO_2, CO, SO_2, NH_3, H_2S, HCN, HF, CH_4, N_2, and H_2) on the pure and Pd-decorated GeS_2 (Pd-GeS_2) monolayers were performed by using first-principles calculations to explore the viability of the GeS_2 monolayers as gas sensors for NO_x detection. Our study indicates that the pristine GeS_2 monolayer physically adsorbs gas molecules and has a rather fast recovery time, implying that the pure GeS_2 monolayer is unfit for gas sensor manufacturing. Pd decoration then was used to modulate the adsorption behaviors of molecules on the GeS_2 surface. The Pd atoms are impossible to aggregate on the monolayer that was confirmed by the binding energy per Pd atom and transition state theory. The decorated Pd atoms can notably increase the adsorption strength of gases. Further analysis of the adsorption energy, charge transfer, change in electronic and optical properties, and recovery time of molecules adsorbed on the Pd-GeS_2 monolayers reveal that the Pd-GeS_2 monolayers are promising candidate materials for achieving the selective and sensitive detection of NO_2 and NO gases. Overall, this work can provide some guidance for experiments to further investigate the applications of GeS_2 monolayers in gas sensing.

2. COMPUTATIONAL METHODS

All geometric structures and electronic properties of (Pd-decorated) GeS_2 monolayers adsorbed with molecules were calculated using the spin-polarized density functional theory (DFT) method accomplished in the DMol^3 package.[42,43] The Perdew−Burke−Ernzerhof (PBE)[44] form of the generalized gradient approximation (GGA) functional with van der Waals corrections of Grimme scheme (DFT-D2 method)[45] was used in this work. The related atomic parameters (C_6 and R_0) in Grimme scheme used here were placed in Table S1 in Supporting Information, and the Grimme scheme parameters *s*6 and *d* were set to be 0.75 and 20.0, respectively. The double numerical atomic orbitals with *d*-polarization functions (DNP basis set) and the DFT semicore pseudopotential (DSPP)[46] were selected. We noted that the DSPP approximation used in DMol^3 package has introduced some degree of scalar relativistic corrections into the core which has been proved to be a very well behaved pseudopotential.[47] The Brillouin zone was represented by Monkhorst−Pack meshes[48] of 10 × 10 × 1 *k*-points. The Hirshfeld method[49] was used to calculate the transferred charge. All structure optimizations were accomplished until the energy was less than 1.0×10^{-6} Ha and the force less than 0.002 Ha/Å. For all calculations, the thickness of the space vacuum was set to 20 Å to avoid interactions between periodic images. The electron localization function (ELF) implemented in the CASTEP package[50] was used to describe the bonding features in the system. The cutoff energy of the plane wave was set to 500 eV. To evaluate the energetic stability of Pd atom binding with the GeS_2 monolayer, we defined the binding energy as follows:

$$E_b = E_{Pd-GeS2} - E_{GeS2} - E_{Pd} \quad (1)$$

where $E_{Pd\text{-}GeS2}$, E_{GeS2}, and E_{Pd} denote the total energy of Pd-decorated GeS_2 monolayers, the pure GeS_2 monolayers, and isolated Pd atom, respectively. A negative E_b value indicates that the decoration process of Pd atoms on GeS_2 monolayers is exothermic and energetically favorable. We also calculated the adsorption energy (E_{ad}) of molecules on GeS_2 monolayers with and without Pd decoration using the following equation:

$$E_{ad} = E_{total} - E_{mono} - E_{mol} \quad (2)$$

where E_{total}, E_{mono}, and E_{mol} denote the total energies of the molecule−monolayer adsorption system, (Pd-decorated) GeS_2 monolayer, and the single gas molecule, respectively.

3. RESULTS AND DISCUSSION

3.1. Structural and Electronic Properties of Molecules on the Pure GeS_2 Monolayer. Figure 1a presents the optimized configuration of the 4 × 4 × 1 supercell of the GeS_2 monolayer containing 16 Ge and 32 S atoms. The intrinsic GeS_2 monolayer has a MoS_2-like ABA structure,[51] formed by a layer of Ge atoms intercalated into two layers of S atoms, where each sulfur atom directly bonded to the Ge atom, and the top view resembles the staggered formation of a two-layer graphene structure. This structure corresponds to a single slab of the high-pressure, layer-structured, tetragonal CdI_2-type phase.[40,41] To determine the equilibrium lattice parameters of the GeS_2 monolayer, the total energy of the 4 × 4 × 1 supercell of the monolayer as a function of the lattice constant was calculated and is shown in Figure 1b. We found that the GeS_2 monolayer possesses a symmetry group of $P\bar{3}m1$ with the lattice constants of $a = b = 3.416$ Å, which is slightly smaller than previous reports (3.45 Å).[39−41] The Ge−S bond length in the GeS_2 monolayer is 2.44 Å, which is very different from that

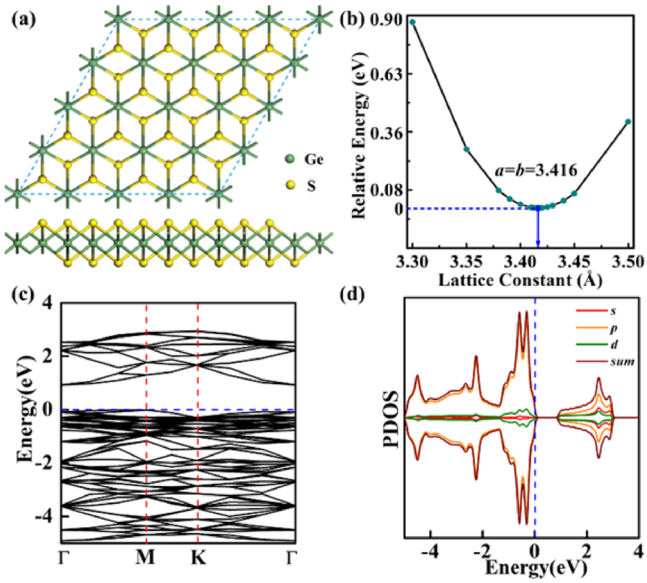

Figure 1. (a) Top- and side-views of the optimized structure for the GeS_2 monolayer, (b) the relative total energy over the lattice constant, the minimum was set to 0 eV, (c and d) the BS and PDOS of the GeS_2 monolayer. Ge and S atoms are in green and yellow balls, respectively.

https://doi.org/10.1021/acsomega.2c05142
ACS Omega 2022, 7, 46440−46451

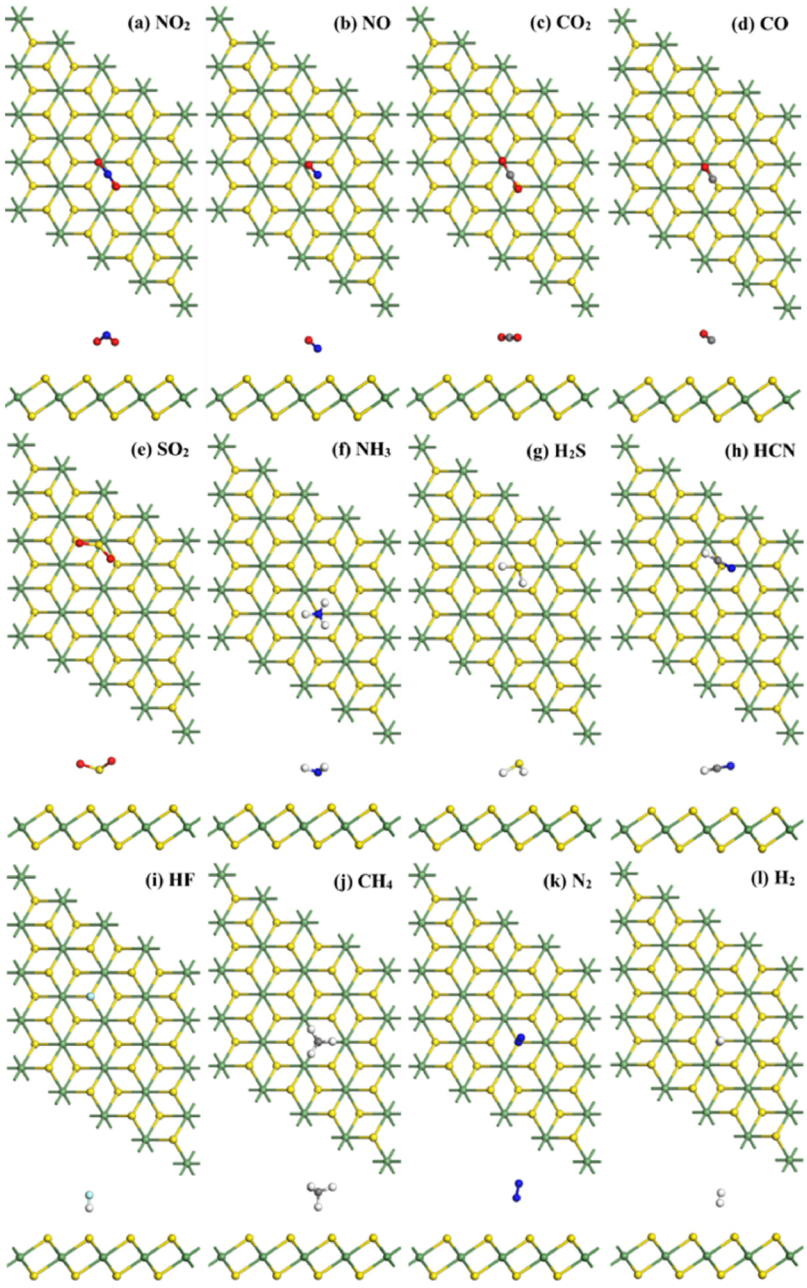

Figure 2. Top- and side-views of the most stable configurations of the pure GeS_2 monolayer interacting with molecules ((a) NO_2, (b) NO, (c) CO_2, (d) CO, (e) SO_2, (f) NH_3, (g) H_2S, (h) HCN, (i) HF, (j) CH_4, (k) N_2, and (l) H_2). O, N, C, F, and H atoms are represented in red, blue, gray, cyan, and white balls, respectively.

of the GeS monolayer[34] in which two types of Ge−S bond lengths are found (2.37 and 2.47 Å). The electronic properties (band structure (BS) and partial density of states (PDOS)) of the GeS_2 monolayer in Figure 1c,d showed that it is a nonmagnetic semiconductor with a band-gap width of 0.93 eV, which is in good agreement with previous work.[39−41] It should be emphasized that although the PBE method we used underestimates the band gap width of the GeS_2 monolayer, which was reported to be 1.47 eV by using the HSE06 functional,[39] in this work what we mainly focus on is the change of the band gap before and after molecular adsorption, which will determine the sensitivity of the gas sensor. The change trends in the band gap of the different semiconductor energies obtained by the PBE and HSE06 functional are consistent.[52,53]

In order to probe into the gas-sensing performance of the pristine GeS_2 monolayer, we considered different adsorption sites (such as top, bridge, and hollow sites) of several gases (NO_2, NO, CO_2, CO, SO_2, NH_3, H_2S, HCN, HF, CH_4, N_2, and H_2) on the GeS_2 monolayer and the orientation of molecules referring to the substrate surface for constructing as many as possible initial adsorption structures. After full optimization of these initial structures, we obtained the most stable configurations of molecules on the GeS_2 monolayer, which are displayed in Figure 2. We found that NO_2, CO, NO, CO_2, and SO_2 molecules are all located above the top site of the Ge atom, and NH_3, H_2S, HCN, CH_4, N_2, and H_2 are located above the hollow site of the Ge−S six-membered ring, while the HF molecule is erected above the top site of one S atom. The corresponding calculated results are summarized in

https://doi.org/10.1021/acsomega.2c05142
ACS Omega 2022, 7, 46440−46451

Table 1. The adsorption of NO and NH_3 possesses the strongest adsorption behavior (-0.4 eV < E_{ad} < -0.3 eV),

Table 1. Adsorption Energy (E_{ad}), the Shortest Distance (D) and Charge Transfer (Q) from Molecule to Monolayer, Band Gap (E_g), and Recovery Time (τ) for Molecules on the GeS_2 Monolayer

system	E_{ad} (eV)	D (Å)	Q (e)	E_g (eV)	τ (s)
GeS_2				0.93	
NO_2	−0.23	2.72	−0.02	0.68	7.99×10^{-9}
NO	−0.38	2.38	0.14	metallic	2.64×10^{-6}
CO_2	−0.18	3.02	−0.03	0.93	9.32×10^{-10}
CO	−0.14	2.98	−0.02	0.93	2.19×10^{-10}
SO_2	−0.21	2.88	−0.07	0.93	3.87×10^{-9}
NH_3	−0.33	2.57	0.05	0.78	3.05×10^{-7}
H_2S	−0.23	2.86	−0.02	0.44	6.52×10^{-9}
HCN	−0.19	3.02	−0.04	0.93	1.85×10^{-9}
HF	−0.25	2.24	−0.13	0.93	1.52×10^{-8}
CH_4	−0.15	2.27	−0.06	0.93	2.82×10^{-10}
N_2	−0.13	2.97	−0.01	0.93	1.63×10^{-10}
H_2	−0.11	2.50	−0.04	0.93	7.14×10^{-11}
HCHO	−0.19	3.02	−0.06	0.44	1.75×10^{-9}

while the other molecule adsorption has a much smaller adsorption energy. The very weak adsorption strength, the large distance between the molecule and monolayer, and small charge transfer lead to the inability to form chemical bonds, and it is thus predicted that the GeS_2 monolayer physically adsorbs all the molecules. However, a significant redistribution of the charge of the GeS_2 monolayer occurs because of the NO and HF adsorption. According to the Hirshfeld method analysis, the NO molecule is an acceptor that received 0.14 e of charge and the HF molecule is a donor that provided 0.13 e of charge from/to the GeS_2 monolayer, respectively. The described charge redistribution and transfer due to gas adsorption is expected to play a major role in the current−voltage characteristics. Due to the charge transfer between the molecule and GeS_2, we can obtain the resistivity change of the material experimentally and therefore can exploit it in gas sensors.[54−56] Since formaldehyde (HCHO) is also a kind of hazardous indoor gas dangerous to human health, we also considered the possibility of the GeS_2 monolayer as an HCHO sensor. The most stable configuration of HCHO on the monolayer is shown in Figure S1 in the Supporting Information. We found that the HCHO molecule is located at the center of the pore of the monolayer, similar to the cases of other molecules, and physisorbed on the monolayer due to the quite small adsorption energy, large distance, and unobvious charge transfer as shown in Table 1.

We plotted the density of states (DOS) of molecules adsorbed on GeS_2 along with the local DOS (LDOS) of molecules in Figure 3 to facilitate a deep understanding of the variation in the electronic properties of the GeS_2 monolayers due to molecule adsorption. According to the analysis of the data in Table 1, the adsorption of molecules does not change the band-gap value of the GeS_2 monolayer except for NO_2, NH_3, and H_2S for which the band-gap value was decreased from 0.93 to 0.68, 0.78, and 0.44 eV, respectively. The change of DOS for the adsorption of HCHO on the GeS_2 monolayer is similar to that of the H_2S molecule. In particular, the adsorption of NO makes the semiconducting properties of the monolayer change into conducting properties, where the band gap is zero. Further, the adsorption of NO_2 and NO introduces a total magnetic moment of 1 μ_B in the system and induces impurity states near the Fermi level, resulting in a reduction of the band gap as shown in Figure 3. The pure GeS_2 monolayer is known to be nonmagnetic, and the adsorption of NO and

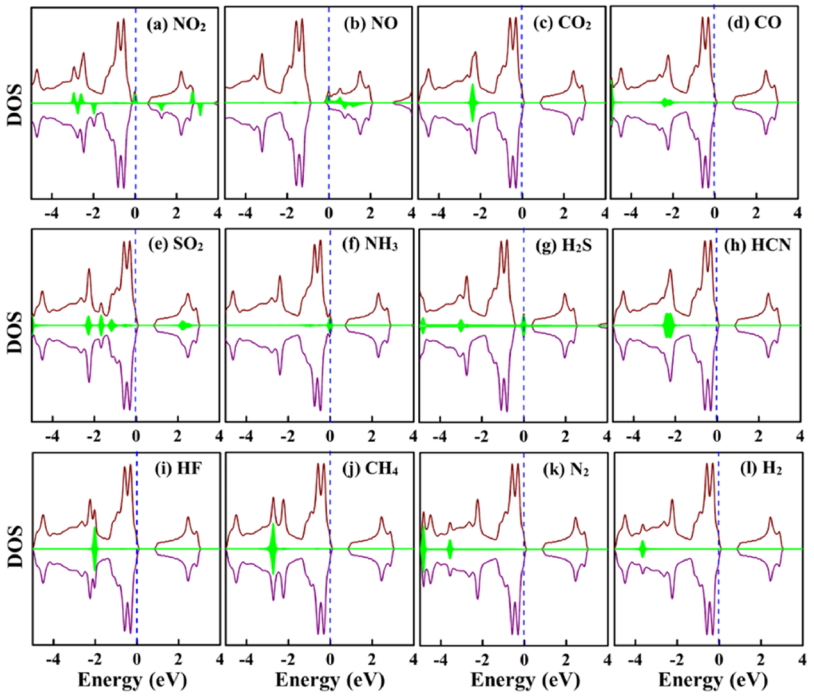

Figure 3. DOSs of molecules ((a) NO_2, (b) NO, (c) CO_2, (d) CO, (e) SO_2, (f) NH_3, (g) H_2S, (h) HCN, (i) HF, (j) CH_4, (k) N_2, and (l) H_2) adsorbed on the GeS_2. Fermi level, majority-spin, and minority-spin states are displayed as blue, wine, and purple lines, respectively, and the LDOS of molecules is shown in the green filled area.

https://doi.org/10.1021/acsomega.2c05142
ACS Omega 2022, 7, 46440−46451

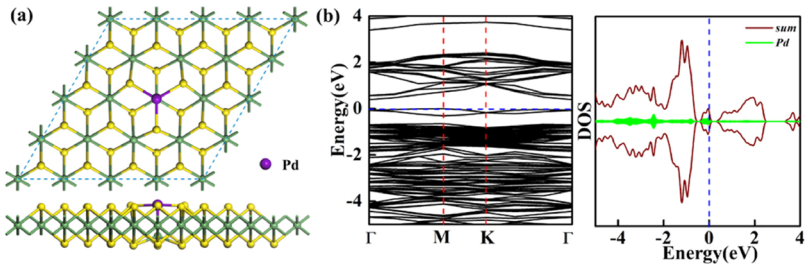

Figure 4. (a) Top- and side-views of the Pd-GeS_2 structure and (b) the corresponding BS and DOS. Purple ball represents the Pd atom.

NO_2 molecules brings magnetism into the GeS_2 monolayer, which would be used to develop a new high-sensitive gas detection technique by measuring the local magnetic moments of GeS_2 monolayers using various experimental techniques such as SQUID magnetometer or magnetic atomic force microscopy.[57]

These results indicate that the pure GeS_2 monolayer is highly sensitive to NO_2, NO, NH_3, and H_2S gases, and it seems that the pure GeS_2 monolayer should be suitable for the detection of these gases. However, to be a good gas sensor, the desorption of a molecule from the gas sensor would be befitting, that is, the recovery time of the gas sensor would be moderate, which is the time for molecule desorption from the monolayer, and also means the time that the molecule can stay on the monolayer. The recovery time (τ) is described as the van't-Hoff–Arrhenius expression:[58]

$$\tau = \nu_0^{-1} e^{-E_{ad}/kT} \quad (3)$$

where ν_0 is the attempt frequency of each molecule that can be assumed to be 10^{12} s^{-1} as NO_2 molecule.[59] We then could predict the recovery times of the pure GeS_2 monolayer for different gases at 300 K, and the results are shown in Table 1. In addition, the relevant calculated data of recovery times are summarized in Table S2 of Supporting Information. Although the adsorption of NO has the largest adsorption energy of −0.38 eV among molecule adsorption, the corresponding recovery time of 2.64×10^{-6} s at 300 K is too short to measure, and thereby causes the device to fail to detect these gases within the effective times. In this context, the pure GeS_2 monolayer is not applicable as a gas sensor for the considered gas detection. To enable the GeS_2 monolayer appropriate for gas sensing, the primary task is to enhance the adsorption strength of molecules on the GeS_2 monolayer, and consequently increase the recovery time, and even enhance the sensitivity and selectivity.

3.2. Modification of the GeS_2 Monolayer with Pd Decoration. Metal decoration and defects are the most common means of modulating material properties. For example, TM dopants can effectively modify the chemical activity and electron mobility of materials,[60] and thereby enhance the gas molecule adsorption strength and gas-sensing properties of monolayers.[61−64] Although defects may improve the sensing performance of GeS_2 monolayers, analysis of the adsorption strength of gases on other TMD materials with defects shows that defects can largely enhance the adsorption strengths of gases on the surfaces that makes gas desorption quite difficult and thus the recovery times are too long,[65,66] so here we only considered the effect of decoration on the sensing performance of GeS_2 monolayers. To further improve the feasibility of the GeS_2 monolayer as gas sensors, we then focused on the effect of Pd decoration. The selected dopant, Pd, has attracted much attention for enhancing the gas-sensing properties of 2D nanomaterials, which is mainly because that (i) the d orbitals of Pd atoms play an important part in the gas interactions with the substrate, that is, the hybridization between the d orbitals of Pd atoms and molecular orbitals would be intensified, which would further strengthen drastically the electron redistribution, and accordingly make the gas response much faster and the recovery time much more moderate, as accomplished in other 2D nanomaterials;[67−69] (ii) the monolayer with Pd dopants can be realized by methods such as ion beam modification[70] and electron-beam mediated substitutional doping approach;[71] (iii) the electronic and optical properties of 2D nanomaterials such as BS, charge transfer, and work function can be significantly improved by Pd doping.[72−74]

The optimized Pd-decorated GeS_2 (Pd-GeS_2) monolayer remains largely in the original structural form of the pure monolayer, and the Pd atom lies at the top position of one Ge. The introduction of Pd atom causes the Ge atom below the adsorption site to sink slightly, forming an S−Pd bond of 2.33 Å (consistent with the S−Pd bond length in the $Pd_3P_2S_8$ crystal[75]) and a Ge−Pd bond of 2.34 Å (similar to the Ge−Pd bond length in the dipalladium complex[76]), as shown in Figure 4a. The covalent functionalization has an important effect on the stabilities and BSs of the TMDs, which in turn determines the gas-sensitive mechanism of the sensor. Pd atoms transfer their electrons to the unoccupied states of the GeS_2 during decoration, thus imparting stability to the material, and the net charge transfer during adsorption also supports strong chemisorption.[77] Therefore, it is crucial to determine the changes in the electronic properties of GeS_2 with Pd decoration. Due to its nonmagnetic nature, we only plotted the spin-up BS of the Pd-GeS_2 system in Figure 4b, and it can be found that the conduction band bottom and valence band top are located at the Γ and *M* points, respectively, and the system has no states across the Fermi energy level, even with the introduction of Pd atoms. Its total DOS plotted in Figure 4b shows that the impurity states produced by Pd atoms make the Fermi level move to conduction bands, and the hybridization between Pd atoms and the monolayer promotes the Pd atoms to transfer 0.3 *e* electrons to the GeS_2 monolayer to form a positively charged Pd dopant and induce a strong chemical bond between the dopant and the GeS_2 monolayer with a binding energy (E_b) of −4.01 eV. These results suggest that the Pd doping does not change the semiconductor properties of the GeS_2 monolayer as an indirect band-gap semiconductor. However, the calculated band gap was reduced from 0.93 eV for the GeS_2 monolayer to 0.39 eV, which could be attributed to the activation of the bottom of the conduction band and the top of the valence band by the dopant.[78]

https://doi.org/10.1021/acsomega.2c05142
ACS Omega 2022, 7, 46440−46451

The stability of the Pd-GeS_2 monolayer was also carried out. The binding energy of the Pd atom (−4.01 eV) is close to the polymerization energy of the Pd metal (−3.9 eV), so we focused on the possible polymerization behaviors of Pd on the GeS_2 monolayer, which were investigated via the complete linear/quadratic synchronous transit method.[79] Considering that only the top site of Ge atom is the most favorable position for Pd atoms, the potential pathway of Pd atoms from one of the most stable sites (as initial structure, IS) to another one (as final structure, FS) was considered as shown in Figure 5, where

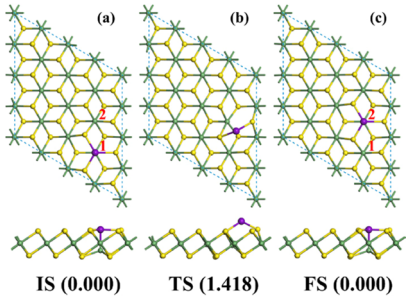

Figure 5. Pathway from (a) one site (initial structure (IS)) of the most stable state to (c) another site (final structure (FS)), (b) the transition state (TS). Energies (in eV) of the IS, TS, and FS states are shown relative to the total energy of IS state.

the Pd atom locates at site 1 in the IS state while it locates at site 2 in FS. The results show that the energy barrier of Pd atom moving from site 1 to site 2 is 1.418 eV with a TS (confirmed by one imaginary frequency of −64.9 cm^{-1}) locating at the top of one S atom shown in Figure 5b, which means that the diffusion of Pd atoms on the GeS_2 monolayer is too difficult and the modification process of Pd atoms on the GeS_2 surface would avoid the clustering of Pd atoms.

To further assess the stability of the Pd-GeS_2 monolayer, we investigated the thermodynamic properties of the Pd-GeS_2 monolayer. First-principles Born−Oppenheimer molecular dynamics (BOMD) simulations of the structure of the Pd-GeS_2 monolayer in an *NVT* ensemble were performed. We used a Nose−Hoover thermostat chain to control the temperature, which is 300 K in this work. The combination of GGA-PBE and DNP was used for BOMD simulations. The total simulation time was set to 6 ps and the corresponding time step was 1 fs. Figure 6 shows the total energy variation of the structure during the simulation. Within 6 ps, we do not observe any deformation of the Pd-GeS_2 structure, as the

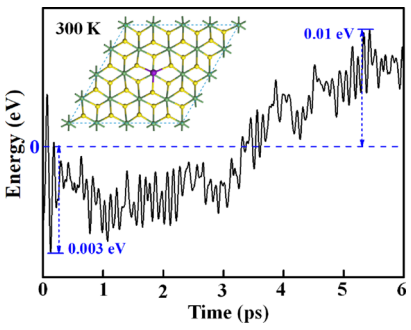

Figure 6. Total energy (eV) of the Pd-GeS_2 monolayer over time at 300 K. Figure inset is the structure of the Pd-GeS_2 monolayer after 6 ps simulation.

energy of the Pd-GeS_2 monolayer oscillates around the same energy value during the simulation (the range of energy <0.01 eV). This fact supports the calculated thermodynamic stability of the Pd-GeS_2 monolayer.

3.3. Adsorption and Gas-Sensing Properties of Molecules on the Pd-GeS_2 Monolayer. We then studied the adsorption of common gases (NO_2, NO, CO_2, CO, SO_2, NH_3, H_2S, HCN, HF, CH_4, N_2, and H_2) on the Pd-GeS_2 monolayer, and their most optimal adsorption structures are displayed in Figure 7. It is clear that, on the whole, the doping of Pd makes the adsorption energy of all gases increase to different degrees, and the structure of the Pd-GeS_2 monolayer remains unchanged after the adsorption of gases.

The NO_2 molecule adsorbs on the Pd-GeS_2 monolayer with an E_{ad} of −0.53 eV, and the interaction between NO_2 and Pd-GeS_2 results in the formation of a chemical O−Pd bond of 2.30 Å. The O−N−O bond angle in NO_2 is also reduced from 133° to 125°. In this process, NO_2 also acts as an acceptor to receive a charge of 0.13 *e* from the Pd-GeS_2 monolayer, so we predict that NO_2 is weakly chemisorbed on the Pd-GeS_2. To further elucidate the chemisorption of NO_2, its ELF was calculated and is presented in Figure 8a. It is clear that the interaction between O in NO_2 and Pd atom has the nature of ionic bonds, indicating the chemisorption of NO_2 on the monolayer. The adsorption of NO and CO has significantly higher adsorption energies than NO_2 (−0.83 and − 1.01 eV, respectively), which indicates that NO and CO are more chemically adsorbed on the Pd-GeS_2 monolayer than NO_2. The ELF plots as presented in Figure 8b,d further proved this conclusion. Interestingly, the charge transfer between the NO (or CO) and the monolayer was much smaller than that of NO_2, where it is transferred 0.03 *e* (or 0.02 *e*) of charge from NO (or CO) to Pd-GeS_2. According to Figure 8b, the charge density of N atom in NO clearly shows an asymmetric distribution, which is due to the interaction between N and Pd atoms with an ELF value of about 0.5, forming an N−Pd bond of 2.08 Å. Similar features were found in the case of CO adsorption. The S atom of SO_2 is located directly above the Pd atom, leading to a Pd−S bond of 2.38 Å. The O−S bond length and the O−S−O bond angle in SO_2 still remain at 1.48 Å and 120°, respectively. Considering the E_{ad} of SO_2 (−0.55 eV) and the inconspicuous charge transfer between SO_2 and the Pd-GeS_2 monolayer (0.06 *e*), we presume that it adsorbs on the Pd-GeS_2 monolayer in the form of weak chemisorption, confirmed further from ELF plots shown in Figure 8e. For HCHO adsorbed on the Pd-GeS_2 monolayer as shown in Figure S1, HCHO behaves similarly to that of SO_2 molecule. According to the data in Table 2, NH_3, H_2S, and HCN are adsorbed on the Pd-GeS_2 monolayer with adsorption energies of −1.32, −0.91, and − 0.75 eV, respectively, and none of the charge transfer amounts are less than 0.1 *e* (0.18, 0.17, and 0.13 *e*, respectively). It is easy to see from Figure 8 that NH_3 and the substrate forms an ionic N−Pd bond with a length of 2.25 Å, and the adsorption of H_2S forms an ionic S−Pd bond of 2.54 Å, and HCN is adsorbed vertically above the Pd atom, forming an ionic N−Pd bond of 2.18 Å. It is obvious that NH_3, H_2S, and HCN are strongly chemisorbed on the Pd-GeS_2 monolayer. Since the adsorption energies of CO_2, HF, CH_4, N_2, and H_2 are less than −0.4 eV and the charge transfer is less than 0.05 *e*, there is no strong interaction between these five gases and the Pd-GeS_2 monolayer, so it is confirmed that these five gases are physically adsorbed on the Pd-GeS_2 monolayer.

https://doi.org/10.1021/acsomega.2c05142
ACS Omega 2022, 7, 46440−46451

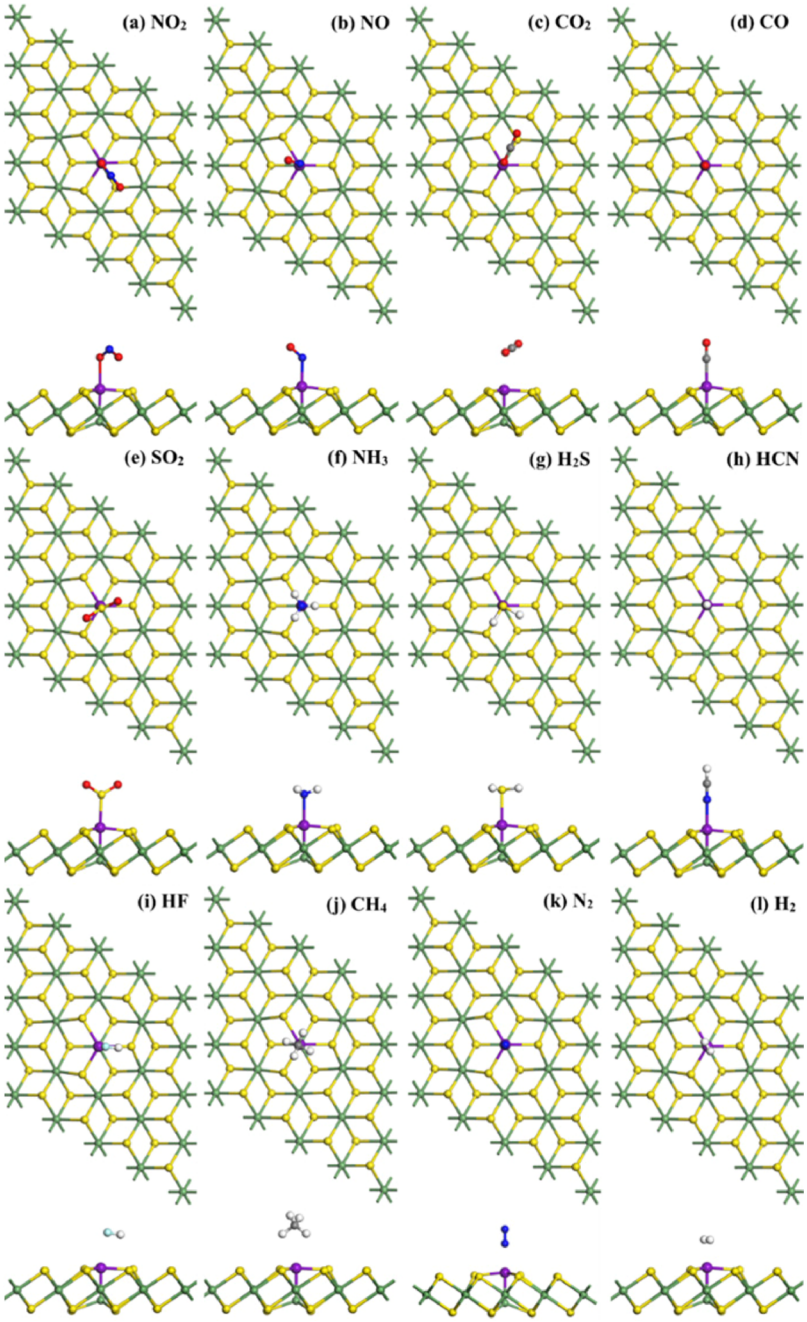

Figure 7. Top- and side-views of the most stable configurations for molecules ((a) NO_2, (b) NO, (c) CO_2, (d) CO, (e) SO_2, (f) NH_3, (g) H_2S, (h) HCN, (i) HF, (j) CH_4, (k) N_2, and (l) H_2) on the Pd-GeS_2 monolayer.

According to the DOSs of NO_2 and NO adsorption on the Pd-GeS_2 monolayer as shown in Figure 9a,b, the spin-up and spin-down DOSs are asymmetric in the same energy range, indicating that the magnetic moments of 1 μ_B were introduced by the adsorption of NO_2 and NO. The introduction of impurity states due to NO_2 and NO adsorption, which are quite close to the Fermi level, reduces greatly the band-gap value (0.39 eV) of the Pd-GeS_2 monolayers to 0.18 and 0.22 eV, respectively. In other words, the Pd-GeS_2 monolayer can achieve the selective and specific sensing of NO_2 and NO because of the increased conductivity of the monolayer. In contrast, the adsorption of the other gas molecules does not produce magnetic moments. The main contributions introduced by the other molecules are the mainly produced occupied state in the valence band or the unoccupied state in the conduction band, or both that are all far away from the Fermi level, which makes the band-gap widths of the Pd-GeS_2 monolayer slightly enlarged as shown in Table 2.

The primary factor for gas-sensitive and trapping materials is their gas sensitivity (S), which is usually assessed as follows:[80]

$$S = \frac{R_g - R_p}{R_p} \times 100\% \quad (4)$$

where R_g and R_p are the sensor resistance after and before molecule adsorption, respectively. It is known that the resistance (R) expresses a reciprocal relationship to conductivity (σ) as shown:

https://doi.org/10.1021/acsomega.2c05142
ACS Omega 2022, 7, 46440−46451

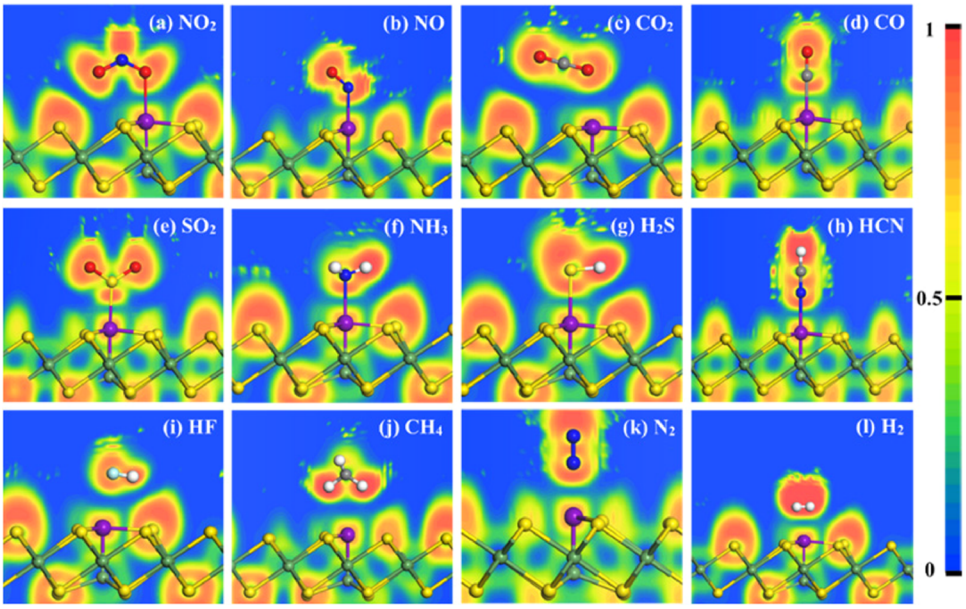

Figure 8. ELF plots of molecules ((a) NO_2, (b) NO, (c) CO_2, (d) CO, (e) SO_2, (f) NH_3, (g) H_2S, (h) HCN, (i) HF, (j) CH_4, (k) N_2, and (l) H_2) adsorbed on the Pd-GeS_2 monolayer.

Table 2. Adsorption Energy (E_{ad}), the Shortest Distance (D) and Charge Transfer (Q) from Molecule to Monolayer, Band Gap (E_g), and Recovery Time (τ) for Gases on the Pd-GeS_2 Monolayer

system	E_{ad} (eV)	D (Å)	Q (e)	E_g (eV)	τ (s)
Pd-GeS_2				0.39	
NO_2	−0.53	2.30	−0.13	0.18	7.82×10^{-4}
NO	−0.83	2.08	0.03	0.22	81.8
CO_2	−0.26	2.72	0.01	0.42	2.63×10^{-8}
CO	−1.01	2.01	0.02	0.65	1.02×10^{5}
SO_2	−0.55	2.38	−0.06	0.62	1.83×10^{-3}
NH_3	−1.32	2.25	0.18	0.53	12.4×10^{10}
H_2S	−0.91	2.54	0.17	0.54	2.24×10^{3}
HCN	−0.75	2.18	0.13	0.53	4.31
HF	−0.36	2.60	−0.002	0.43	1.32×10^{-6}
CH_4	−0.30	2.64	−0.05	0.42	9.13×10^{-8}
N_2	−0.37	2.23	0.04	0.54	1.51×10^{-6}
H_2	−0.29	2.04	−0.002	0.52	8.06×10^{-8}
HCHO	−0.69	2.33	0.08	0.48	3.57×10^{-1}

$$R = \frac{1}{\sigma} \tag{5}$$

where the conductivity (σ) of semiconductors is obtained from the formula:[81]

$$\sigma = AT^{3/2}\exp\left(\frac{-E_g}{2kT}\right) \tag{6}$$

where A, T, and k denote the certain constant, temperature, and Boltzmann constant, respectively. It can be seen from the above equations that the widened band-gap widths of materials would reduce the electrical conductivity of the Pd-GeS_2 monolayer and increase the corresponding electrical resistance after interaction with these molecules. On the contrary, the narrowed band-gap widths due to molecule adsorption can make the carrier transition easier and increase the electrical conductivity and thereby decrease the corresponding resistance, which is desirable for gas-sensing materials.[82−84] The calculated sensitivity of the Pd-GeS_2 monolayer toward NO_2 and NO gases is 98.3 and 96.3%, respectively, indicating that the high sensitivity of the Pd-GeS_2 monolayer toward NO_2 and NO gases. To further investigate the coverage effect of gases on the Pd-GeS_2 monolayer, we used the Pd-GeS_2 structure with different supercells ($3 \times 3 \times 1$, $4 \times 4 \times 1$, and $5 \times 5 \times 1$) to regulate the coverage of adsorbed gases. We just considered the coverage effects of NO_2 and NO gases as examples, and the corresponding most stable structures with different supercells are shown in Figure S2, and the related results are summarized in Table S3. In the most stable structure of the molecule on the Pd-GeS_2 monolayer with different supercells, the (NO_2 and NO) molecule is located at the top of the Pd atom. Moreover, the adsorption energy in different coverage is almost the same as shown in Table S3, and the electronic properties remain almost unchanged except for NO with high coverage. We found that when the NO molecule is adsorbed on the small supercell, the band gap is decreased. In addition, in order to distinguish these two gases in the mixture containing NO_2 and NO, we calculated the work functions of NO_2 and NO adsorbed on the Pd-GeS_2 monolayer as 6.15 and 5.85 eV, respectively, while the work function of the pure Pd-GeS_2 monolayer is 6.04 eV. The work functions of the two gases show an increasing and decreasing trend, respectively, which will facilitate us to distinguish NO_2 and NO.

It is obvious from eq 3 that the recovery time of the Pd-GeS_2 monolayer toward NO_2 and NO gases at T = 300 K is 0.782 ms and 81.8 s (the calculated data of recovery time are shown in Table S4 in Supporting Information), respectively, which are quite moderate for detecting both NO_2 and NO gases, as it is superior to other 2D TMDs,[30,85] For example, the 2D MoS_2-based good gas sensors have been reported to show recovery times as long as about 100 s.[86] In addition, the recovery time of CO, NH_3, and H_2S on the Pd-GeS_2 monolayer is significantly too long, which in turn brings about the problem of difficult gas desorption, and in this regard, it may be inappropriate to use the Pd-GeS_2 monolayer-based sensor for the detection of CO, NH_3, and H_2S. In contrast, the recovery time of CO_2, HCN, HF, CH_4, N_2, and H_2 is too short to be difficult to

https://doi.org/10.1021/acsomega.2c05142
ACS Omega 2022, 7, 46440−46451

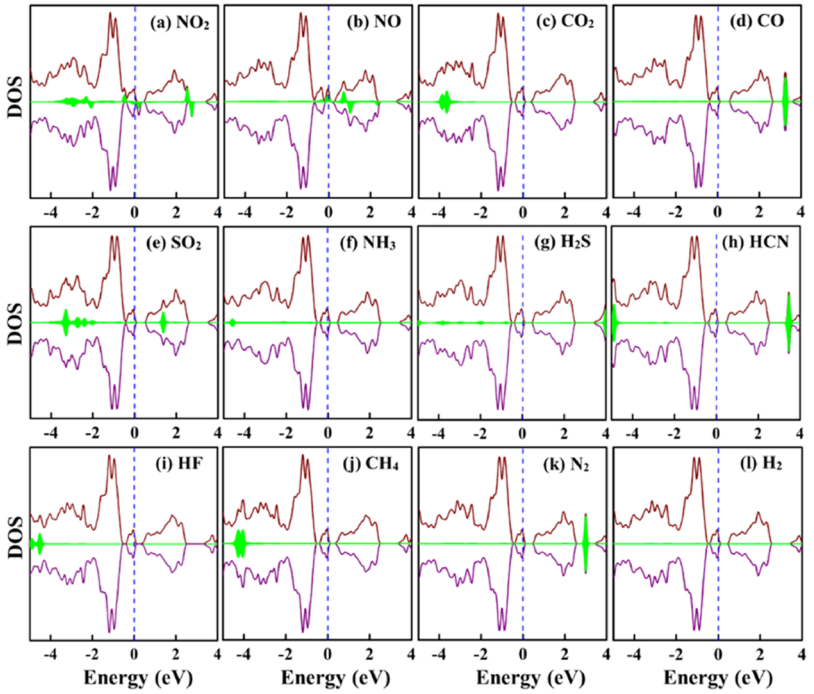

Figure 9. DOSs of molecules ((a) NO_2, (b) NO, (c) CO_2, (d) CO, (e) SO_2, (f) NH_3, (g) H_2S, (h) HCN, (i) HF, (j) CH_4, (k) N_2, and (l) H_2) adsorbed on the Pd-GeS_2 monolayer. Fermi level, majority-spin, and minority-spin states are displayed as blue, wine, and purple lines, respectively, and the LDOS of molecules is shown in green filled area.

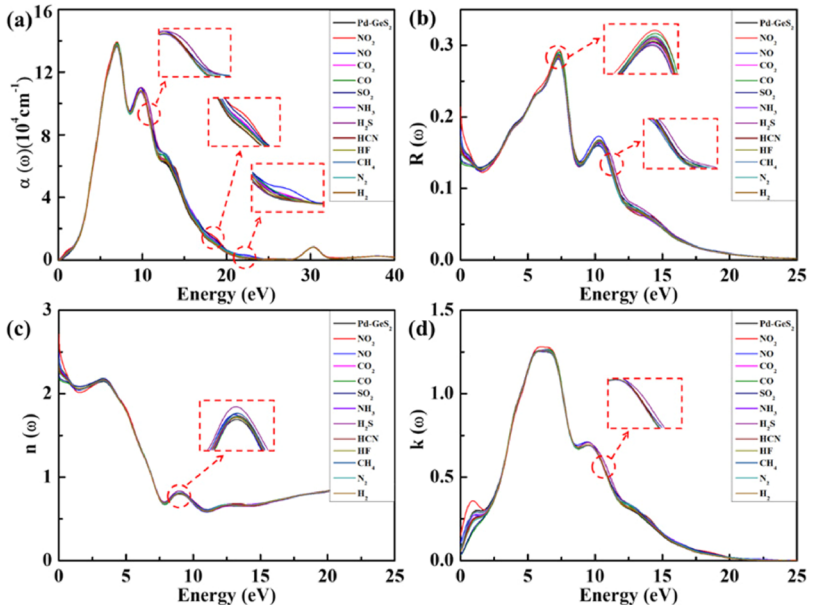

Figure 10. (a) Absorption coefficient (α), (b) the reflectivity (Re), (c) and (d) the real (n) and imaginary (k) part of the refractive index of pristine and gas molecules adsorbed on the Pd-GeS_2 monolayer. Dashed rectangles in the figures are the enlarged part of curves in the dashed circles.

measure. Therefore, the Pd-GeS_2 monolayer is a promising candidate for reusable gas sensors to monitor NO and NO_2 at room temperature.

The difference in the optical properties of different gases adsorbed on the sensing material can be used to distinguish the type of gases.[87−89] We thus further studied the optical properties such as absorption coefficient, reflectivity, and refractive index of the Pd-GeS_2 monolayer with adsorbed molecules to explore its potential application in optical gas sensors, as shown in Figure 10. As presented in Figure 10a, the absorption capacity of the Pd-GeS_2 monolayer is enhanced between 10.16 and 11.32 eV by the adsorption of H_2S molecules, in addition, after the adsorption of NO_2, the absorption values are changed remarkably around 18.57 eV (66.77 nm), and they are changed obviously near 22.38 eV (55.41 nm) due to the adsorption of NO, which suggest that the Pd-GeS_2 monolayer could differentiate different gases under different frequencies, and is potentially attractive for photovoltaic applications due to the adsorption of NO_2 and NO. From the reflectance (Re) curves of the Pd-GeS_2

https://doi.org/10.1021/acsomega.2c05142
ACS Omega 2022, 7, 46440−46451

monolayer with molecular adsorption, as shown in Figure 10b, we found that in the vacuum UV region, the two systems of adsorbed NO_2 and NO occupy the highest reflectance peaks at 7.32 eV (169.40 nm) and 10.24 eV (121.09 nm), respectively, and H_2S can significantly enhance the reflectance of the Pd-GeS_2 monolayer when the energy is higher than 10.84 eV (114.39 nm). At energies below 0.89 eV in the infrared region, the reflectivity of the NO_2 system is enhanced, while the reflectivity of CO and SO_2 is lower than that of the pure Pd-GeS_2 monolayer. As shown in Figure 10c,d, the adsorption of NO_2 has a significant effect on the refractive index of the Pd-GeS_2 monolayer in both IR and UV regions, while the changes in the enhanced refractive index caused by the adsorption of H_2S are mainly present in the vacuum UV region. From the above analysis, we found that the changes in the optical properties of the Pd-GeS_2 monolayer mainly originate from the adsorption of NO_2, NO, and H_2S, while the effects of CO and SO_2 mainly occur in the IR region.

4. CONCLUSIONS

In summary, we explored the geometries and electronic, optical, and gas-sensing properties of various gases (NO_2, NO, CO_2, CO, SO_2, NH_3, H_2S, HCN, HF, CH_4, N_2, and H_2) on the (Pd-decorated) GeS_2 monolayers via spin-polarized DFT methods. We found the pure GeS_2 monolayers only interact physically with gases and these gases cannot influence the electronic properties of the monolayer except for NO. The NO adsorption induces significant charge transfer and change of electronic properties, but its over-rapid recovery time (2.64×10^{-6} s) severely hinders the application of the GeS_2 monolayer as a NO gas sensor. To improve the adsorption strength, we considered Pd atoms decorated on the GeS_2 monolayer and determined its structural stability via binding energy, TS theory, and MD simulations. We further found that the Pd decoration significantly increases the adsorption strength of the GeS_2 monolayer interacting with gas molecules, and in return the adsorption of molecules dramatically affects the electronic and optical properties of the Pd-GeS_2 monolayer. The Pd-decorated GeS_2 monolayer is highly sensitive to NO and NO_2 gases. The recovery time of NO and NO_2 is moderate for molecule desorption and is suitable for reuse of the device. Further, the adsorption of NO and NO_2 can remarkably modify the optical properties of the Pd-GeS_2 monolayers, so that we can differentiate the NO and NO_2 from the considered gases using the change of optical properties induced by molecule adsorption. Therefore, it is predicted that the Pd-GeS_2 monolayers are reusable and highly sensitive (optical) gas sensors for NO_2 and NO detection.

■ ASSOCIATED CONTENT

Supporting Information

The Supporting Information is available free of charge at https://pubs.acs.org/doi/10.1021/acsomega.2c05142.

Detailed data of Grimme's D2 scheme, calculated recovery time, and molecules on the monolayers with different supercells (PDF)

■ AUTHOR INFORMATION

Corresponding Author

Yongliang Yong − *School of Physics and Engineering, Henan Key Laboratory of Photoelectric Energy Storage Materials and Applications, Henan University of Science and Technology, Luoyang 471023, China; Longmen Laboratory, Luoyang, Henan 471003, China;* orcid.org/0000-0001-7376-0738; Email: ylyong@haust.edu.cn

Authors

Ruilin Gao − *School of Physics and Engineering, Henan Key Laboratory of Photoelectric Energy Storage Materials and Applications, Henan University of Science and Technology, Luoyang 471023, China*

Xiaobo Yuan − *School of Physics and Engineering, Henan Key Laboratory of Photoelectric Energy Storage Materials and Applications, Henan University of Science and Technology, Luoyang 471023, China*

Song Hu − *School of Physics and Engineering, Henan Key Laboratory of Photoelectric Energy Storage Materials and Applications, Henan University of Science and Technology, Luoyang 471023, China*

Qihua Hou − *School of Physics and Engineering, Henan Key Laboratory of Photoelectric Energy Storage Materials and Applications, Henan University of Science and Technology, Luoyang 471023, China*

Yanmin Kuang − *Institute of Photobiophysics, School of Physics and Electronics, Henan University, Kaifeng 475004, China*

Complete contact information is available at: https://pubs.acs.org/10.1021/acsomega.2c05142

Author Contributions

The manuscript was written through contributions of all authors. All authors have given approval to the final version of the manuscript.

Notes

The authors declare no competing financial interest.

■ ACKNOWLEDGMENTS

This work is supported by the National Natural Science Foundation of China (No. 61774056 and 12004101) and the Young Backbone Teacher in Colleges and Universities of Henan Province (Grant No. 2020GGJS076).

■ REFERENCES

(1) Schwierz, F. Graphene transistors: Status, prospects, and problems. *Proc. IEEE* **2013**, *101*, 1567−1584.

(2) Schwierz, F.; Pezoldt, J.; Granzner, R. Two-dimensional materials and their prospects in transistor electronics. *Nanoscale* **2015**, *7*, 8261−8283.

(3) Liu, Z. K.; Lau, S. P.; Yan, F. Functionalized graphene and other two-dimensional materials for photovoltaic devices: Device design and processing. *Chem. Soc. Rev.* **2015**, *44*, 5638−5679.

(4) Shen, J. H.; Zhu, Y. H.; Yang, X. L.; Li, C. Z. Graphene quantum dots: Emergent nanolights for bioimaging, sensors, catalysis and photovoltaic devices. *Chem. Commun.* **2012**, *48*, 3686−3699.

(5) Bie, C. B.; Yu, H. G.; Cheng, B.; Ho, W.; Fan, J. J.; Yu, J. G. Design, fabrication, and mechanism of nitrogen-doped graphene-based photocatalyst. *Adv. Mater.* **2021**, *33*, No. 2003521.

(6) Bie, C. B.; Zhu, B. C.; Xu, F. Y.; Zhang, L. Y.; Yu, J. G. In situ grown monolayer N-doped graphene on CdS hollow spheres with seamless contact for photocatalytic CO_2 reduction. *Adv. Mater.* **2019**, *31*, No. 1902868.

(7) Xu, H. F.; Ma, L. B.; Jin, Z. Nitrogen-doped graphene: Synthesis, characterizations and energy applications. *J. Energy Chem.* **2018**, *27*, 146−160.

(8) Yong, Y. L.; Cui, H. L.; Zhou, Q. X.; Su, X. Y.; Kuang, Y. M.; Li, X. H. C_2N monolayer as NH_3 and NO sensors: A DFT study. *Appl. Surf. Sci.* **2019**, *487*, 488−495.

(9) Zhao, Z. J.; Yong, Y. L.; Hu, S.; Li, C. T.; Kuang, Y. M. Adsorption of gas molecules on a C_3N monolayer and the implications for NO_2 sensors. *AIP Adv.* **2019**, *9*, 125308.
(10) Hu, S.; Yong, Y. L.; Li, C. T.; Zhao, Z. J.; Jia, H. W.; Kuang, Y. M. Si_2BN monolayers as promising candidates for hydrogen storage. *Phys. Chem. Chem. Phys.* **2020**, *22*, 13563−13568.
(11) Zhao, Z. J.; Yong, Y. L.; Zhou, Q. X.; Kuang, Y. M.; Li, X. H. Gas-sensing properties of the SiC monolayer and bilayer: A density functional theory study. *ACS Omega* **2020**, *5*, 12364−12373.
(12) Hu, S.; Yong, Y. L.; Zhao, Z. J.; Gao, R. L.; Zhou, Q. X.; Kuang, Y. M. C_7N_6 monolayer as high capacity and reversible hydrogen storage media: A DFT study. *Int. J. Hydrogen Energy* **2021**, *46*, 21994−22003.
(13) Wang, X. J.; Yong, Y. L.; Yang, W. W.; Zhang, A. D.; Xie, X. Y.; Zhu, P.; Kuang, Y. M. Adsorption, gas-sensing, and optical properties of molecules on a diazine monolayer: A first-principles study. *ACS Omega* **2021**, *6*, 11418−11426.
(14) Yong, Y. L.; Hu, S.; Zhao, Z. J.; Gao, R. L.; Cui, H. L.; Lv, Z. L. Potential reversible and high-capacity hydrogen storage medium: Li-decorated B_3S monolayers. *Mater. Today Commun.* **2021**, *29*, No. 102938.
(15) Yong, Y. L.; Ren, F. F.; Zhao, Z. J.; Gao, R. L.; Hu, S.; Zhou, Q. X.; Kuang, Y. M. Highly enhanced NH_3-sensing performance of BC_6N monolayer with single vacancy and stone-wales defects: A DFT study. *Appl. Surf. Sci.* **2021**, *551*, No. 149383.
(16) Zhao, Z. J.; Yong, Y. L.; Gao, R. L.; Hu, S.; Zhou, Q. X.; Su, X. Y.; Kuang, Y. M.; Li, X. H. Adsorption, sensing and optical properties of molecules on BC_3 monolayer: First-principles calculations. *Mater. Sci. Eng., B* **2021**, *271*, No. 115266.
(17) Zhao, Z. J.; Yong, Y. L.; Gao, R. L.; Hu, S.; Zhou, Q. X.; Kuang, Y. M. Enhancement of nitride-gas sensing performance of SiC_7 monolayer induced by external electric field. *Vacuum* **2021**, *191*, No. 110393.
(18) Yong, Y. L.; Gao, R. L.; Yuan, X. B.; Zhao, Z. J.; Hu, S.; Kuang, Y. M. Gas sensing and capturing based on the C_7N_6 monolayer with and without metal decoration: A first-principles investigation. *Appl. Surf. Sci.* **2022**, *591*, No. 153129.
(19) Cui, H.; Zhang, G. Z.; Zhang, X. X.; Tang, J. Rh-doped $MoSe_2$ as a toxic gas scavenger: A first-principles study. *Nanoscale Adv.* **2019**, *1*, 772−780.
(20) Chang, K.; Hai, X.; Ye, J. H. Transition metal disulfides as noble-metal-alternative Co-catalysts for solar hydrogen production. *Adv. Energy Mater.* **2016**, *6*, No. 1502555.
(21) Shi, Y. M.; Li, H. N.; Li, L. J. Recent advances in controlled synthesis of two-dimensional transition metal dichalcogenides via vapour deposition techniques. *Chem. Soc. Rev.* **2015**, *44*, 2744−2756.
(22) Wang, Q. H.; Kalantar-Zadeh, K.; Kis, A.; Coleman, J. N.; Strano, M. S. Electronics and optoelectronics of two-dimensional transition metal dichalcogenides. *Nat. Nanotechnol.* **2012**, *7*, 699−712.
(23) Brent, J. R.; Savjani, N.; O'Brien, P. Synthetic approaches to two-dimensional transition metal dichalcogenide nanosheets. *Prog. Mater. Sci.* **2017**, *89*, 411−478.
(24) Wang, Y.; Chhowalla, M. Making clean electrical contacts on 2D transition metal dichalcogenides. *Nat. Rev. Phys.* **2022**, *4*, 101−112.
(25) Raju, P.; Li, Q. Review-Semiconductor materials and devices for gas sensors. *J. Electrochem. Soc.* **2022**, *169*, No. 057518.
(26) Zhang, J.; Liu, X. H.; Neri, G.; Pinna, N. Nanostructured materials for room-temperature gas sensors. *Adv. Mater.* **2016**, *28*, 795−831.
(27) Jian, Y. Y.; Hu, W. W.; Zhao, Z. H.; Cheng, P. F.; Haick, H.; Yao, M. S.; Wu, W. W. Gas sensors based on chemi-resistive hybrid functional nanomaterials. *Nano-Micro Lett.* **2020**, *12*, 71.
(28) Kumar, R.; Liu, X. H.; Zhang, J.; Kumar, M. Room-temperature gas sensors under photoactivation: From metal oxides to 2D materials. *Nano-Micro Lett.* **2020**, *12*, 164.
(29) Yong, Y. L.; Gao, R. L.; Wang, X. J.; Yuan, X. B.; Hu, S.; Zhao, Z. J.; Li, X. H.; Kuang, Y. M. Highly sensitive and selective room-temperature gas sensors based on $B_6N_6H_6$ monolayer for sensing SO_2 and NH_3: A first-principles study. *Res. Phys.* **2022**, *33*, No. 105208.
(30) Kim, T. H.; Kim, Y. H.; Park, S. Y.; Kim, S. Y.; Jang, H. W. Two-dimensional transition metal disulfides for chemoresistive gas sensing: Perspective and challenges. *Chemosensors* **2017**, *5*, 15.
(31) Li, Q.; Meng, J. P.; Li, Z. Recent progress on Schottky sensors based on two-dimensional transition metal dichalcogenides. *J. Mater. Chem. A* **2022**, *10*, 8107−8128.
(32) Wang, B. R.; Gu, Y.; Chen, L.; Ji, L.; Zhu, H.; Sun, Q. Q. Gas sensing devices based on two-dimensional materials: A review. *Nanotechnology* **2022**, *33*, 252001.
(33) Zheng, L.; Wang, X. W.; Jiang, H. J.; Xu, M. Z.; Huang, W.; Liu, Z. Recent progress of flexible electronics by 2D transition metal dichalcogenides. *Nano Res.* **2022**, *15*, 2413−2432.
(34) Gao, R. L.; Yong, Y. L.; Hu, S.; Zhao, Z. J.; Li, X. H.; Kuang, Y. M. Adsorption and gas-sensing performance of SF_6 decomposition gases on GeS monolayers with and without single vacancies and Si-doping. *Appl. Surf. Sci.* **2021**, *568*, No. 150961.
(35) Panigrahi, P.; Hussain, T.; Karton, A.; Ahuja, R. Elemental substitution of two-dimensional transition metal dichalcogenides ($MoSe_2$ and $MoTe_2$): Implications for enhanced gas sensing. *ACS Sens.* **2019**, *4*, 2646−2653.
(36) Kaur, S. P.; Hussain, T.; Kumar, T. J. D. Substituted 2D Janus WSSe monolayers as efficient nanosensor toward toxic gases. *J. Appl. Phys.* **2021**, *130*, No. 014501.
(37) Panigrahi, P.; Panda, P. K.; Pal, Y.; Bae, H.; Lee, H.; Ahuja, R.; Hussain, T. Two-dimensional bismuthene nanosheets for selective detection of toxic gases. *ACS Appl. Nano Mater.* **2022**, *5*, 2984−2993.
(38) Singh, A.; Bae, H.; Hussain, T.; Watanabe, H.; Lee, H. Efficient sensing properties of aluminum nitride nanosheets toward toxic pollutants under gated electric field. *ACS Appl. Nano Mater.* **2020**, *2*, 1645−1652.
(39) Wang, X. L.; Feng, W.; Shen, C.; Sun, Z. H.; Qi, H. B.; Yang, M.; Liu, Y. H.; Wu, Y. C.; Wu, X. Q. The verification of thermoelectric performance obtained by high-throughput calculations: The case of GeS_2 monolayer from first-principles calculations. *Front. Mater.* **2021**, *8*, No. 709757.
(40) Yang, Y. S.; Liu, S. C.; Wang, X.; Li, Z. B.; Zhang, Y.; Zhang, G. M.; Xue, D. J.; Hu, J. S. Polarization-sensitive ultraviolet photodetection of anisotropic 2D GeS_2. *Adv. Funct. Mater.* **2019**, *29*, No. 1900411.
(41) Sarikurt, S.; Kocabaş, T.; Sevik, C. High-throughput computational screening of 2D materials for thermoelectrics. *J. Mater. Chem. A* **2020**, *8*, 19674−19683.
(42) Delley, B. An all-electron numerical method for solving the local density functional for polyatomic molecules. *J. Chem. Phys.* **1990**, *92*, 508−517.
(43) Delley, B. From molecules to solids with the $Dmol^3$ approach. *J. Chem. Phys.* **2000**, *113*, 7756−7764.
(44) Perdew, J. P.; Burke, K.; Ernzerhof, M. Generalized gradient approximation made simple. *Phys. Rev. Lett.* **1996**, *77*, 3865−3868.
(45) Grimme, S. Semiempirical GGA-type density functional constructed with a long-range dispersion correction. *J. Comput. Chem.* **2006**, *27*, 1787−1799.
(46) Hamann, D. R.; Schluter, M.; Chiang, C. Norm-conserving pseudopotentials. *Phys. Rev. Lett.* **1979**, *43*, 1494−1497.
(47) Delley, B. Hardness conserving semilocal pseudopotentials. *Phys. Rev. B: Condens. Matter Mater. Phys.* **2002**, *66*, No. 155125.
(48) Monkhorst, H. J.; Pack, J. D. Special points for Brillouin-zone integrations. *Phys. Rev. B: Condens. Matter Mater. Phys.* **1977**, *16*, 1748−1749.
(49) Hirshfeld, F. L. Bonded-atom fragments for describing molecular charge densities. *Theor. Chim. Acta* **1977**, *44*, 129−138.
(50) Clark, S. J.; Segall, M. D.; Pickard, C. J.; Hasnip, P. J.; Probert, M. I. J.; Refson, K.; Payne, M. C. First principles methods using CASTEP. *Z. Kristallogr.* **2005**, *220*, 567−570.
(51) Ding, G. Q.; Gao, G. Y.; Huang, Z. S.; Zhang, W. X.; Yao, K. L. Thermoelectric properties of monolayer MSe_2 (M=Zr, Hf): Low

https://doi.org/10.1021/acsomega.2c05142
ACS Omega 2022, 7, 46440−46451

lattice thermal conductivity and a promising figure of merit. *Nanotechnology* **2016**, *27*, No. 375703.
(52) Heyd, J.; Peralta, J. E.; Scuseria, G. E.; Martin, R. L. Energy band gaps and lattice parameters evaluated with the Heyd-Scuseria-Ernzerhof screened hybrid functional. *J. Chem. Phys.* **2005**, *123*, 174101.
(53) Janesko, B. G.; Henderson, T. M.; Scuseria, G. E. Screened hybrid density functionals for solid-state chemistry and physics. *Phys. Chem. Chem. Phys.* **2009**, *11*, 443−454.
(54) Zhang, X. X.; Sun, J. H.; Tang, K. S.; Wang, H. R.; Chen, T. T.; Jiang, K. S.; Zhou, T. Y.; Quan, H.; Guo, R. H. Ultralow detection limit and ultrafast response/recovery of the H_2 gas sensor based on Pd-doped rGO/ZnO-SnO_2 from hydrothermal synthesis. *Microsyst. Nanoeng.* **2022**, *8*, 67.
(55) Cho, B.; Hahm, M. G.; Choi, M.; Yoon, J.; Kim, A. R.; Lee, Y. J.; Park, S. G.; Kwon, J. D.; Kim, C. S.; Song, M.; Jeong, Y.; Nam, K. S.; Lee, S.; Yoo, T. J.; Kang, C. G.; Lee, B. H.; Ko, H. C.; Ajayan, P. M.; Kim, D. H. Charge-transfer-based gas sensing using atomic-layer MoS_2. *Sci. Rep.* **2015**, *5*, 8052.
(56) Wang, J.; Yang, G. F.; Xue, J. J.; Lei, J. M.; Cai, Q.; Chen, D. J.; Lu, H.; Zhang, R.; Zheng, Y. D. High sensitivity and selectivity of AsP sensor in detecting SF_6 decomposition gases. *Sci. Rep.* **2018**, *8*, 12011.
(57) Zanolli, Z.; Charlier, J. C. Single-molecule sensing using carbon nanotubes decorated with magnetic clusters. *ACS Nano* **2012**, *6*, 10786−10791.
(58) Zhang, Y.; Chen, Y.; Zhou, K.; Liu, C.; Zeng, J.; Zhang, H.; Peng, Y. Improving gas sensing properties of graphene by introducing dopants and defects: A first-principles study. *Nanotechnology* **2009**, *20*, No. 185504.
(59) Peng, S.; Cho, K.; Qi, P.; Dai, H. Ab initio study of CNT NO_2 gas sensor. *Chem. Phys. Lett.* **2004**, *387*, 271−276.
(60) Ma, D. W.; Ju, W. W.; Li, T. X.; Zhang, X. W.; He, C. Z.; Ma, B. Y.; Tang, Y. N.; Lu, Z. S.; Yang, Z. X. Modulating electronic, magnetic and chemical properties of MoS_2 monolayer sheets by substitutional doping with transition metals. *Appl. Surf. Sci.* **2016**, *364*, 181−189.
(61) Ma, D. W.; Ju, W. W.; Li, T. X.; Zhang, X. W.; He, C. Z.; Ma, B. Y.; Lu, Z. S.; Yang, Z. X. The adsorption of CO and NO on the MoS_2 monolayer doped with Au, Pt, Pd, or Ni: A first-principles study. *Appl. Surf. Sci.* **2016**, *383*, 98−105.
(62) Zhang, D.; Wu, J.; Peng, L.; Cao, Y. Room-temperature SO_2 gas-sensing properties based on a metal-doped MoS_2 nanoflower: An experimental and density functional theory investigation. *J. Mater. Chem. A* **2017**, *5*, 20666−20677.
(63) Lu, Z. S.; Lv, P.; Ma, D. W.; Yang, X. W.; Li, S.; Yang, Z. X. Detection of gas molecules on single Mn adatom adsorbed graphene: A DFT-D study. *J. Phys. D: Appl. Phys.* **2018**, *51*, No. 065109.
(64) Ma, D. W.; Ju, W. W.; Li, T. X.; Yang, G.; He, C. Z.; Ma, B. Y.; Tang, Y. N.; Lu, Z. S.; Yang, Z. X. Formaldehyde molecule adsorption on the doped monolayer MoS_2: A first-principles study. *Appl. Surf. Sci.* **2016**, *371*, 180−188.
(65) Agrawal, A. V.; Kumar, N.; Kumar, M. Strategy and future prospects to develop room-temperature-recoverable NO_2 gas sensor based on two-dimensional molybdenum disulfide. *Nano-Micro Lett.* **2021**, *13*, 38.
(66) Lin, Z.; Carvalho, B. R.; Kahn, E.; Lv, R. T.; Rao, R.; Terrones, H.; Pimenta, M. A.; Terrones, M. Defect engineering of two-dimensional transition metal dichalcogenides. *2D Mater.* **2016**, *3*, No. 022002.
(67) Cui, H.; Jia, P. F.; Peng, X. Y. Adsorption of SO_2 and NO_2 molecule on intrinsic and Pd-doped $HfSe_2$ monolayer: A first-principles study. *Appl. Surf. Sci.* **2020**, *513*, No. 145863.
(68) Ma, S. X.; Li, D. J.; Rao, X. J.; Xia, X. F.; Su, Y.; Lu, Y. F. Pd-doped h-BN monolayer: A promising gas scavenger for SF_6 insulation devices. *Adsorption* **2020**, *26*, 619−626.
(69) Wang, H. W.; Hu, X. X.; Liu, B.; Duan, D. G. Pd-doped SnP_3 monolayer: A new 2D buddy for sensing typical dissolved gases in transformer oil. *Appl. Surf. Sci.* **2021**, *568*, No. 150893.
(70) Li, Z. Q.; Chen, F. Ion beam modification of two-dimensional materials: Characterization, properties, and applications. *Appl. Phys. Rev.* **2017**, *4*, No. 011103.
(71) Komsa, H. P.; Kotakoski, J.; Kurasch, S.; Lehtinen, O.; Kaiser, U.; Krasheninnikov, A. V. Two-dimensional transition metal dichalcogenides under electron irradiation: Defect production and doping. *Phys. Rev. Lett.* **2012**, *109*, No. 035503.
(72) Shi, J.; Quan, W. J.; Chen, X. W.; Chen, X. Y.; Zhang, Y. W.; Lv, W.; Yang, J. H.; Zeng, M.; Wei, H.; Hu, N. T.; Su, Y. J.; Zhou, Z. H.; Yang, Z. Noble metal (Ag, Au, Pd and Pt) doped TaS_2 monolayer for gas sensing: A first-principles investigation. *Phys. Chem. Chem. Phys.* **2021**, *23*, 18359−18368.
(73) Zhu, S. Y.; Ma, S. X. Adsorption and sensing behaviors of Pd-doped InN monolayer upon CO and NO molecules: A first-principles study. *Appl. Sci.* **2019**, *9*, 3390.
(74) Zhou, Q.; Zhang, G.; Tian, S.; Zhang, X. First-principles insight into Pd-doped ZnO monolayers as a promising scavenger for dissolved gas analysis in transformer oil. *ACS Omega* **2020**, *5*, 17801−17807.
(75) Zhang, X.; Luo, Z. M.; Yu, P.; Cai, Y. Q.; Du, Y. H.; Wu, D. X.; Gao, S.; Tan, C. L.; Li, Z.; Ren, M. Q.; Osipowicz, T.; Chen, S. M.; Jiang, Z.; Li, J.; Huang, Y.; Yang, J.; Chen, Y.; Ang, C. Y.; Zhao, Y. L.; Wang, P.; Song, L.; Wu, X. J.; Liu, Z.; Borgna, A.; Zhang, H. Lithiation-induced amorphization of $Pd_3P_2S_8$ for highly efficient hydrogen evolution. *Nat. Catal.* **2018**, *1*, 460−468.
(76) Tanabe, M.; Ishikawa, N.; Osakada, K. Preparation and structure of a new dipalladium complex with bridging diphenylgermyl ligands. Diverse reactivities of $Pd(PCy_3)_2$ and $Pt(PCy_3)_2$ toward Ph_2GeH_2. *Organometallics* **2006**, *25*, 796−798.
(77) John, D.; Nharangatt, B.; Chatanathodi, R. Stabilizing honeycomb borophene by beryllium decoration: a computational study. *J. Mater. Chem. C* **2019**, *7*, 11493−11499.
(78) Ao, Z. M.; Peeters, F. M. High-capacity hydrogen storage in Al-adsorbed graphene. *Phys. Rev. B: Condens. Matter Mater. Phys.* **2010**, *81*, No. 205406.
(79) Govind, N.; Petersen, M.; Fitzgerald, G.; Smith, D. K.; Andzelm, J. A generalized synchronous transit method for transition state location. *Comput. Mater. Sci.* **2013**, *28*, 250−258.
(80) Zhang, X.; Yu, L.; Wu, X.; Hu, W. Experimental sensing and density functional theory study of H_2S and SOF_2 adsorption on Au-modified graphene. *Adv. Sci.* **2015**, *2*, No. 1500101.
(81) Li, S. S.*Semiconductor Physical Electronics*, 2nd edition; Springer: USA, 2006.
(82) Liu, X.; Cheng, S. T.; Liu, H.; Hu, S.; Zhang, D. Q.; Ning, H. S. A survey on gas sensing technology. *Sensors* **2012**, *12*, 9635−9665.
(83) Wang, C. X.; Yin, L. W.; Zhang, L. Y.; Xiang, D.; Gao, R. Metal oxide gas sensors: Sensitivity and influencing factors. *Sensors* **2010**, *10*, 2088−2106.
(84) Kumar, S.; Pavelyev, V.; Mishra, P.; Tripathi, N.; Sharma, P.; Calle, F. A review on 2D transition metal di-chalcogenides and metal oxide nanostructures based NO_2 gas sensors. *Mater. Sci. Semicond. Proc.* **2020**, *107*, No. 104865.
(85) Bhati, V. S.; Kumar, M.; Banerjee, R. Gas sensing performance of 2D nanomaterials/metal oxide nanocomposites: A review. *J. Mater. Chem. C* **2021**, *9*, 8776−8808.
(86) Hashtroudi, H.; Mackinnonb, I. D. R.; Shafiei, M. Emerging 2D hybrid nanomaterials: Towards enhanced sensitive and selective conductometric gas sensors at room temperature. *J. Mater. Chem. C* **2020**, *8*, 13108−13126.
(87) Cui, H.; Yan, C.; Jia, P. F.; Cao, W. Adsorption and sensing behaviors of SF_6 decomposed species on Ni-doped C_3N monolayer: A first-principles study. *Appl. Surf. Sci.* **2020**, *512*, No. 145759.
(88) Cui, H.; Jia, P. F.; Peng, X. Y.; Hu, X. F. Geometric, electronic and optical properties of Pt-doped C_3N monolayer upon NO_x adsorption: A DFT study. *IEEE Sens. J.* **2021**, *21*, 3602−3608.
(89) Zhang, T. T.; Pan, W. F.; Zhang, Z. Y.; Qi, N.; Chen, Z. Q. Theoretical study of small molecules adsorption on pristine and transition metal doped GeSe monolayer for gas sensing application. *Langmuir* **2021**, *38*, 1287−1295.

https://doi.org/10.1021/acsomega.2c05142
ACS Omega 2022, 7, 46440−46451